Received January 12, 2022, accepted February 8, 2022, date of publication February 17, 2022, date of current version February 25, 2022.

Digital Object Identifier 10.1109/ACCESS.2022.3152565

Improving the Sidelobe Level, Return Loss and Bandwidth of Notch-Loaded TM_{30} Mode Patch via Fractal-Slot

ZUBAIR AHMED, AWAB MUHAMMAD, AND MOJEEB BIN IHSAN
Department of Electrical Engineering, National University of Sciences and Technology (NUST), Islamabad 44000, Pakistan
Corresponding author: Zubair Ahmed (zubair.ahmed@ee.ceme.edu.pk)

ABSTRACT This paper presents a method for sidelobe level (SLL) reduction, return loss improvement, and bandwidth enhancement in notch-loaded TM_{30} mode rectangular patch antennas. In this method, a fractal-slot is introduced in the center of notch-loaded patch to remove the unwanted out-of-phase current regions. It is shown that a combination of the fractal-slot and notch loading technique can achieve significant improvement in SLL, return loss, and bandwidth of notch-loaded TM_{30} mode without compromising gain or symmetry of radiation patterns. Moreover, the method also gives an additional degree of freedom to improve the impedance matching without changing the feed location. A prototype of the antenna is fabricated to verify the proposed method. The proposed antenna shows a measured gain of 13 dBi with a low SLL of −16 dB. Furthermore, it shows symmetrical patterns in both planes with cross-polarization (X-pol) levels of less than 35 dB. An under-sampled 4×4 array of the proposed antenna is also presented by utilizing its low SLL property to simplify the complexity of feed networks in high gain array antennas. The array offers the same directivity and SLL as that of an 8×8 array of fundamental mode rectangular patch elements in the same area.

INDEX TERMS Higher order mode patch, TM_{30} mode, high gain antenna, low sidelobe level antenna, undersampled array.

I. INTRODUCTION

Microstrip patch antennas have been extensively used in mobile and satellite communications, Global Positioning Systems and radars due to their attractive features of low profile, ease of fabrication and lightweight. In order to satisfy the resonant condition of half wavelength, rectangular patch antennas are normally operated in their fundamental mode, TM_{10}. However, the TM_{10} mode has an inherent limitation of low gain, which is not optimum to mitigate the propagation losses. Therefore, researchers have proposed different methods to overcome the gain limitation by using array of patches [1]–[2], stack of patches [3]–[4], loading of patches by a superstrate [5]–[9], shunt inductive loading [10]–[11], and higher-order modes [12]–[27].

Higher-order mode patch antennas offer high directivity due to their increased size; however, they suffer from the issues of high SLL in E-plane and inadequate gain. This increase in SLL and inadequate gain is attributed to the significant distance among the inter radiating edges of the patch, due to which the currents undergo 180° phase shift in successive half-cycles. Hence, a non-uniform current distribution with in-phase and out-of-phase regions, as shown in Fig. 1, is produced, which results in grating lobes and inadequate gain.

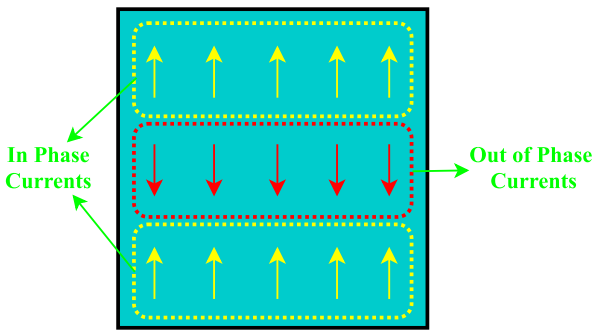

FIGURE 1. Surface currents of a rectangular patch antenna operating in TM_{30} mode.

Over the years, various methodologies have been developed to improve gain and grating lobes of higher-order mode

The associate editor coordinating the review of this manuscript and approving it for publication was Tutku Karacolak.

patch antennas. Some of the commonly used approaches to improve the radiation characteristics include the utilization of high dielectric substrate, the combination of broadside modes, and loading of antennas through slots [12]–[24]. In [12], E-plane SLL of TM_{12} mode circular patch antenna was suppressed by using a high permittivity substrate. Through the utilization of a high dielectric substrate, the overall area of the patch reduces at resonance; however, due to surface wave losses, its radiation efficiency was compromised.

An alternate approach for reducing SLL in higher-order mode patch antennas is to use a linear combination of different broadside modes [13]–[15]. In [13], two circular patch antennas that were operating in two distinct modes are placed one above the other in a stacked configuration. This leads to a dual-mode circular patch antenna in which the lower patch operates in TM_{13} mode while the upper one is in TM_{11} mode. The combination of modes result in reduced SLL and enhanced gain but at the expense of narrow impedance bandwidth and complicated structure. Single-layer implementation of this technique was presented in [14], wherein combination of TM_{12} and TM_{14} modes were demonstrated. Similarly, [15] combines TM_{12} and TM_{14} modes of a circular patch antenna at one frequency, and combines TM_{11} and TM_{13} modes of the same antenna at another frequency. This resulted in a wideband or dual-band circular patch antenna with high gain and low SLL.

Slot loading technique [16]–[24] is another method for enhancing the radiation characteristics in higher-order mode patch antennas. Two reactive slots are placed near radiating edges in [16], to reshape the current distribution of higher-order TM_{30} mode antenna similar to the current distribution of fundamental TM_{10} mode patch antenna. Although the technique eliminated SLL of the higher-order TM_{30} mode patch antenna, but the price paid was degraded gain. In [17], a non-resonant slot-loading technique was used to suppress E-plane SLL of TM_{12} mode circular patch; however, the drawback was high X-pol and asymmetric radiation pattern. To achieve low SLL without compromising X-pol and symmetry of radiation pattern, [18] employed differential feeding for TM_{30} mode slot loaded rectangular patch antenna. The idea of using differential feeding for higher-order mode antennas was further extended in [20] and [21], where a combination of slot and shorting pins were used to achieve dual-band and wideband higher-order mode antennas. In [22], a square patch antenna operating in TM_{03} mode was presented. The antenna consists of three transverse slots and has high gain, low SLL and adjustable beamwidth. Slot loaded TM_{90} mode rectangular patch antenna based dual-polarized, high gain, magnetic antenna array with simple feed network was demonstrated in [23]. In [24], differentially fed circular and rectangular patch antennas loaded with slots and shorting pins were proposed to, respectively, reshape the field distribution of TM_{31} and TM_{12} modes in circular patch antenna, and TM_{21} and TM_{03} modes in rectangular patch antenna. The technique results in antennas with wide bandwidth, enhanced gain, and consistent radiation beamwidth.

In [25], the authors proposed a new technique for gain enhancement and reduction in the E-plane SLL of a higher-order mode patch antenna. Instead of using slots to reshape the out-of-phase currents, removal of out-of-phase regions was proposed for higher-order TM_{30} and TM_{70} mode rectangular patch antennas. This removal, also known as notch-loading, resulted in new in-phase radiating edges and consequently achieved both gain enhancement and SLL reduction. Similar concept with different geometries was also presented in [26] and [27]. In [26], high gain TM_{30} and TM_{50} patch antennas were reported, however, it suffers from high SLL, unsymmetrical patterns and reduced X-pol levels. Theory of Characteristic Modes (TCM) was utilized in [27] to achieve a wide fractional bandwidth; however, the cost was reduced gain.

For the first time, this paper presents a combination of fractal-slot loading technique with notch-loading technique for higher-order mode antennas. The method is applied on a TM_{30} mode rectangular patch antenna and verified by measuring a fabricated prototype of the proposed antenna. The main contributions and salient features of this work are summarized as follows:

1) It is shown that by combining fractal-slot and notch loading technique, the current distribution of higher-order mode patch antennas can be manipulated to achieve low SLL and X-pol without compromising gain and symmetry of the pattern.
2) It is demonstrated that the proposed technique gives an additional degree of freedom for improving the impedance matching and return loss of notch-loaded TM_{30} mode patch antenna.
3) It is shown that the combination of fractal-slot and notch-loading technique can enhance the impedance bandwidth by a factor of 2 when compared to a simple notch-loaded TM_{30} mode patch antenna.
4) An under-sampled high gain, 4×4 array of the proposed antenna is also presented to reduce the complexity of conventional array feed networks.

II. ANTENNA DESIGN AND WORKING PRINCIPLE

This section elaborates on the design of the proposed fractal-slot and notch-loaded patch antenna in detail. After presenting the overall geometry of the antenna, the working principle of fractal-slot loading is explained. Furthermore, an in-depth parametric analysis of fractal-slot dimensions and their effect upon return loss, bandwidth and SLL is also presented in this section.

A. ANTENNA GEOMETRY

Geometry of the proposed fractal-slot and notch-loaded TM_{30} mode rectangular patch antenna is shown in Fig. 2. It comprises of a rectangular patch of length L and width W, which is fed by an SMA connector which is positioned at a distance d_x from the center of the patch. Two notches,

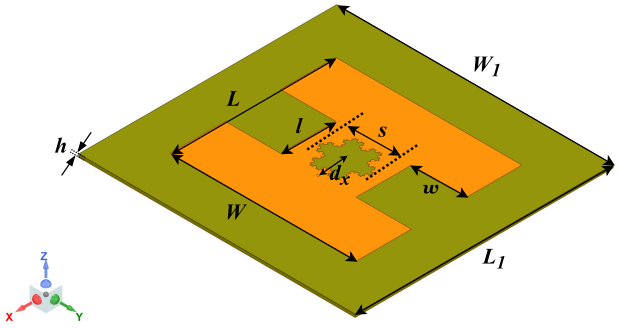

FIGURE 2. Geometry of the proposed design.

each having length l and width w are loaded at the center of both non-radiating edges and a koch fractal-slot is embedded in the center of the antenna. The fractal-slot is obtained by applying three fractal iterations to an equilateral triangle and the fractal slot's maximum dimension is 29 mm. The dimensions of the ground plane are given by $L_1 \times W_1$, where L_1 and W_1 corresponds to the length and the width of the ground plane, respectively. Arlon CuCLad® 217 substrate having relative permittivity of $\epsilon_r = 2.2$ and thickness $h = 1.5$ mm is used for the antenna design. The dimensions of the proposed antenna are $L = 90$ mm, $W = 101$ mm, $l = 30$ mm, $w = 30$ mm, $L_1 = 140$ mm, $W_1 = 150$ mm and $d_x = 15$ mm.

B. WORKING PRINCIPLE

As discussed in Section I, high SLL and inadequate gain in TM_{30} mode patch are due to the presence of unwanted out-of-phase current region. In [25], it is shown that gain can be increased due to the creation of new in-phase radiators between the two radiating edges. Consequently, the SLL is also reduced due to the partial removal of the unwanted current distribution regions. Despite the advantages of the notch-loading technique, the out-of-phase current region still exists, as shown in Fig. 3a, and hence further improvement in SLL is possible. Therefore, this paper proposes a fractal-slot in the out-of-phase current region. The surface current distribution of such design is shown in Fig. 3b for a TM_{30} mode patch antenna. It is worthwhile to note that the fractal-slot only affects the unwanted current distribution, and its effect on the outer desired surface current distribution regions is negligible. Hence, further reduction in SLL can be achieved without compromising the gain.

C. SELECTION OF SLOT SHAPE

In this section, a comparison of three slot shapes, namely, circular, square, and fractal-slots, is presented to determine the optimum slot shape. These different possible slot shapes are shown in Fig. 4. The diameter of the circular slot and side length of the square slot is chosen as 25.8 mm, whereas for the fractal-slot case, the maximum dimension is 29 mm.

The simulated S_{11} of notch-loaded TM_{30} mode antenna with different slot shapes is given in Fig. 5 over the

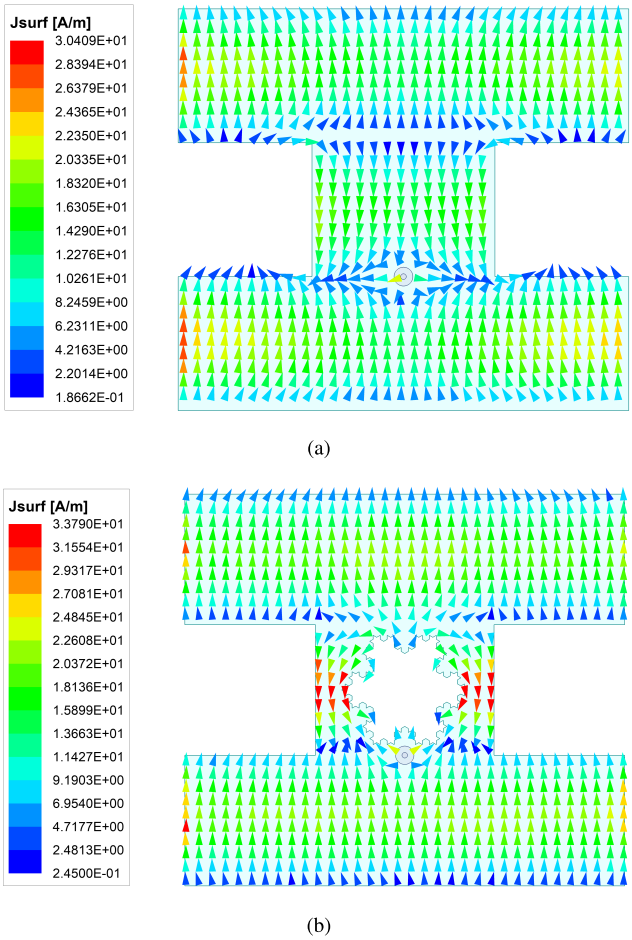

FIGURE 3. Surface currents on notch-loaded TM_{30} patch antenna: (a) without slot, and (b) with fractal-slot.

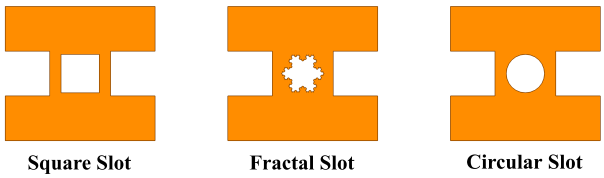

FIGURE 4. Different possible slot shapes.

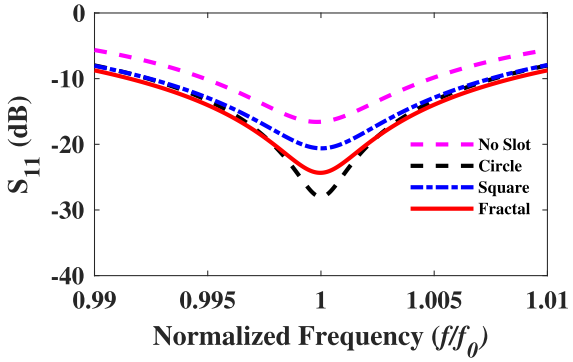

FIGURE 5. S_{11} of different slot shapes.

normalized frequency range. The plot indicates that incorporation of slots improves return loss and bandwidth of

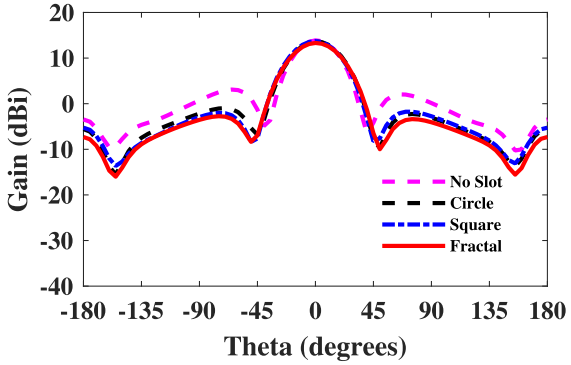

FIGURE 6. E-plane patterns of different slot shapes.

TABLE 1. Comparison with different slot shapes.

Parameters[a]	No Slot	Circular Slot	Fractal Slot	Square Slot
f_0 (GHz)	3.23	3.13	3.09	3.15
RL (dB)	16.2	28	24.3	20.3
BW (MHz)	30	40	60	50
Gain (dBi)	13.9	13.6	13.3	13.7
SLL (dB)	-10.8	-14.6	-16.1	-15.5

[a]f_0= Center Frequency; RL= Return Loss; BW= Bandwidth

notch-loaded TM_{30} mode patch antenna. The fractal slot offers wider bandwidth as compared to circular or square slots. In addition, effect of various slots on the radiation properties of the TM_{30} mode antenna is shown in Fig. 6. It can be observed from the figure that the addition of slot improves the SLL of notch-loaded TM_{30} mode patch antenna. Although the effect of various slot shapes on the SLL of the antenna is similar, the fractal slot offers the lowest SLL.

A more detailed comparison among various antenna parameters of slot shapes is given in Table 1. The introduction of the slot decreases the resonant frequency of the antenna. The currents have to travel an extra distance, reducing the resonant frequency. The fractal-slot has the most significant frequency shift followed, in order, by the circular, square and without slot cases. This decrease in frequency reduces the overall effective area of the antenna as well, due to which a slight reduction in gain can be observed. Moreover, the introduction of the slot improves the original bandwidth of the TM_{30} patch antenna, which is 30 MHz. It is observed that the improvement in bandwidth corresponds to the surface area of the slot. Hence, the fractal-slot shows the maximum increase in bandwidth and has 2 times better bandwidth than the case having no slot. The addition of a slot also improves the SLL of the antenna, and this improvement depends upon the surface area of the slot. The greater the surface area of a slot, the greater the unwanted out-of-phase surface currents removed. Hence, the fractal-slot has the lowest SLL followed, in order, by the square, circular and without slot cases. Based upon the comparison presented in Table 1, a simpler circular or square slot can also be utilized; however, in this paper fractal-slot is selected due to its wider impedance bandwidth and minimum SLL.

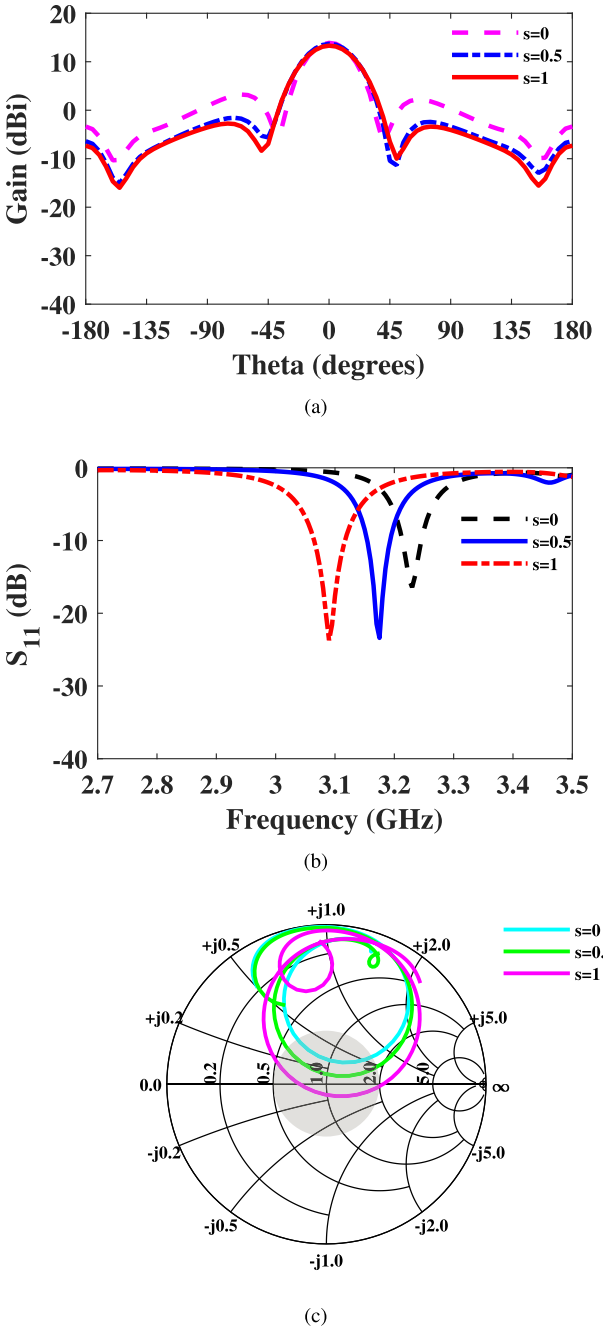

FIGURE 7. Parametric analysis on fractal-slot size: (a) E-plane radiation pattern, (b) return loss, and (c) input impedance.

D. EFFECT OF FRACTAL-SLOT LOADING ON SLL, RETURN LOSS AND BANDWIDTH

The effect of the fractal-slot size on various antenna parameters is shown in Fig. 7. Three normalized slot sizes namely: s = 0, s = 0.5 and s = 1 are investigated. Here, zero slot size represents no fractal-slot loading, i.e., notch-loaded patch without fractal loading. In contrast, a slot size equal to 1 represents the full slot-loading with a maximum dimension of 29 mm.

The effect of fractal-slot size on E-plane SLL is shown in Fig. 7a. The figure shows that by changing the slot size, s, from 0 to 1, E-plane SLL are reduced from −10.8 dB to −16.1 dB. An improvement of about 5.3 dB in SLL is thus achieved using fractal-slot loading. A slight reduction of 0.6 dB in fractal-slot loaded patch antenna gain compared to an antenna without a slot can also be observed. This reduction of antenna gain can be attributed to a decrease in a resonance frequency that decreases the antenna's effective area.

The effect of fractal-slot size on the return loss is shown in Fig. 7b. It can be observed from the figure that an increase in slot size results in a downward shift of resonant frequency from 3.23 GHz to 3.09 GHz. More importantly, impedance matching is also improved with the introduction of the slot. The value of S_{11} changes from −16.2 dB to −24.3 dB by increasing the slot size, s, from 0 to 1. An improvement of around 8.1 dB in S_{11} is achieved by using fractal-slot loading. Thus, introducing fractal-slot adds a new degree of freedom without changing the feed position.

The impedance bandwidth of the antenna, $S_{11} \leq -10$ dB, is also improved to 60 MHz. The fractional bandwidth of TM_{30} mode patch with and without fractal-slot loading is about 1.94% and 0.93%, respectively. Thus, fractal-slot loading also improves the impedance bandwidth of the antenna by a factor of 2.09. To further investigate the reason for impedance bandwidth improvement, the input impedance (Z_{11}) was plotted on Smith Chart for various slot sizes as shown in Fig. 7c. A constant VSWR = 2 circle is also shown in greyish colour for better visualisation. It is worth noting that the increase in slot size increases the loop radius and reduces the antenna's input inductance, which increases impedance bandwidth.

III. RESULTS AND DISCUSSION

The proposed TM_{30} antenna with fractal-slot and notch-loading was fabricated in Microwave Engineering Research Lab (MERL) using an LPKF Protomat H60. Seven holes were drilled near the boundary of the antenna, and an aluminium plate was connected with the ground plane via screws. A 3.5 mm SMA connector was inserted into the metal plate, and its tip was soldered to the top conductor layer. The fabricated antenna is shown in Fig. 8.

The return loss of the fabricated antenna was measured using Agilent E8362B two-port Network Analyzer, and the result is plotted in Fig. 9 along with the simulation results. The measured return loss is 33 dB, compared to the simulated value of 24.3 dB. Measured $S_{11} \leq -10$ dB impedance bandwidth of the antenna is 57 MHz at the center frequency of 3.11 GHz. A slight frequency shift of 20 MHz is also observed between the measured and simulated results, which can be attributed to the fabrication tolerances.

The simulated and measured E- and H-plane radiation patterns are shown in Fig. 10a and Fig. 10b, respectively. A good correlation between the measured and simulated patterns is evident from the figures. The simulated gain of the antenna is 13.3 dBi, whereas the measured gain of the antenna

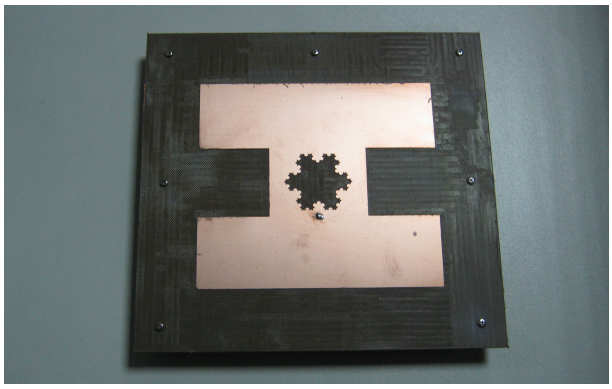

FIGURE 8. Snapshot of the fabricated antenna.

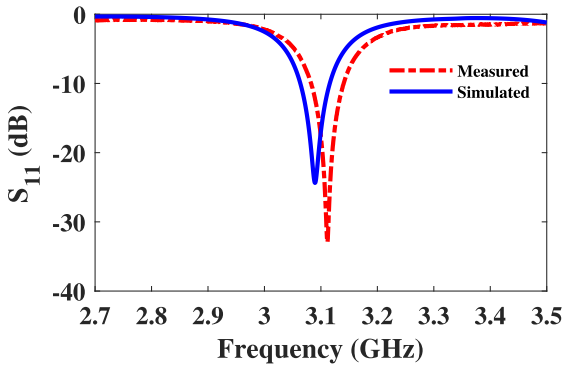

FIGURE 9. Simulated and measured return loss of the antenna.

is 13 dBi, which is 0.3 dB less than the simulated one. The measured E-plane SLL is −16 dB, compared to the simulated value of −16.1 dB. The simulated and the measured H-plane SLL of the antenna are −20.6 dB and −26.2 dB, respectively. The simulated X-pol levels of E- and H-plane are −44 dB and −35 dB, respectively, and measured X-pol levels of E- and H-plane is −41 dB and −33.5 dB, respectively.

In Table 2, the performance of the antenna is compared with the other similar TM_{30} mode patch antennas. Designs of [18] and [24] used differentially fed slots to achieve high gain and low SLL antenna. Due to differential feeding, they have symmetrical patterns with negligible X-pol, but the price paid is an additional and complicated feeding structure. In comparison to [18] and [24], the proposed design offers simple structure with a 3 dB better SLL. Designs of [25]–[27] utilized notch-loading technique. In [26], a maximum gain of 15 dBi is obtained; however, it suffers from unsymmetrical patterns with a high SLL of −6 dB. The X-pol in [26] and [27] is about 18 dB down, whereas the proposed antenna has symmetrical patterns along with a low SLL of −16.1 dB and X-pol of −39 dB. Reference [27] has a good fractional bandwidth of 4.9%, but it has the lowest gain of 10.5 dBi as compared to other designs mentioned in the table. In comparison to [22], the proposed antenna has achieved better gain, aperture efficiency, X-pol level, and fractional bandwidth.

Given the above comparison, the combination of fractal-slot with notch-loading technique in the proposed work has

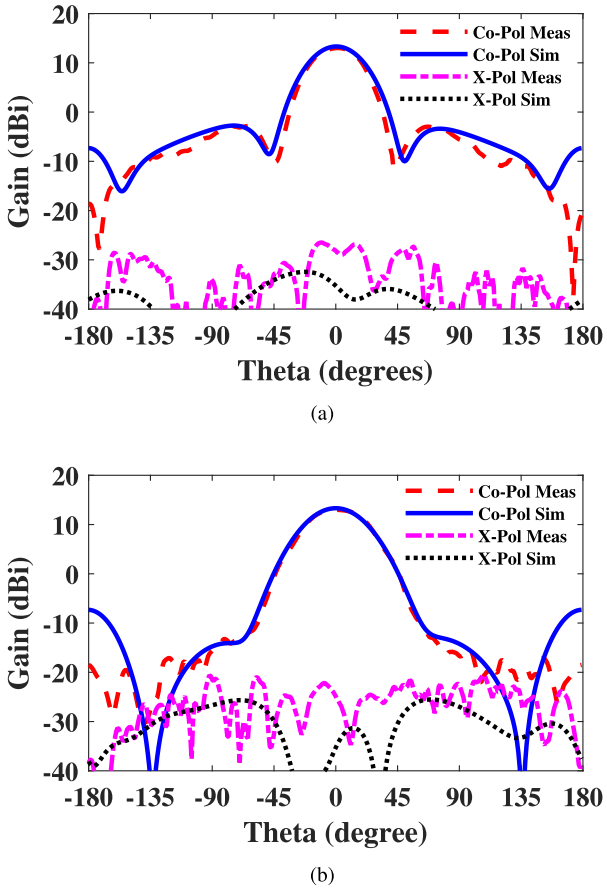

FIGURE 10. Simulated and measured radiation patterns: (a) E-plane and (b) H-plane.

resulted in considerable improvement. The proposed antenna simultaneously offers high gain, low SLL, low X-pol level, and symmetrical radiation patterns without using a complex differential feeding technique.

IV. HIGH GAIN UNDERSAMPLED ARRAY

One of the common approaches to achieving high gain is to make an array of radiators in a linear or planar configuration. Inter-element spacing is a crucial parameter in an array as it determines the mutual coupling between different elements and SLL of the complete array antenna. Moreover, to avoid grating lobes in a uniformly distributed broadside array, a common practice is to select the inter-element distance less than the free-space wavelength (λ_0) [28]. However, [29] showed that grating lobes could be avoided in an undersampled array of higher-order mode fractal antennas.

In this paper, the low SLL property of the proposed antenna is utilized to make a 4×4 array with an inter-element spacing of $1.3\lambda_0$, which is shown in Fig. 11. When compared with a conventional 4×4 array of fundamental mode patch elements with the same inter-element spacing, as shown in Fig. 12, the array of the proposed antenna offers significantly reduced grating lobes.

To explain the underlying principles of the proposed undersampled array, the array factor of a uniform array with

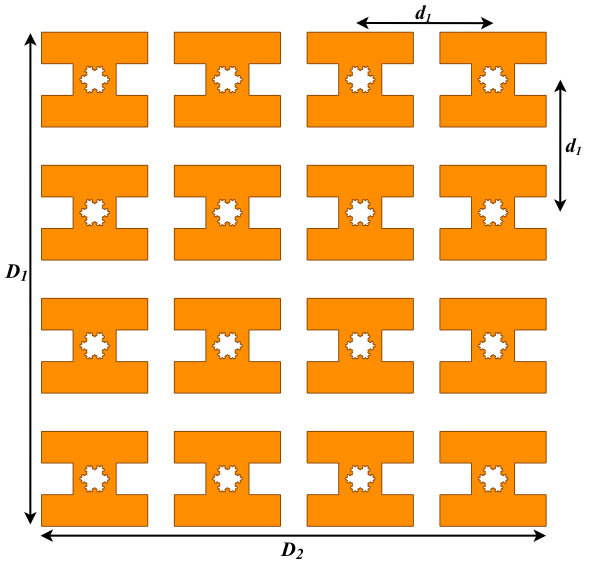

FIGURE 11. 4 × 4 fractal-slot and notch-loaded array with inter-element spacing of $d_1 = 0.64\lambda_0$.

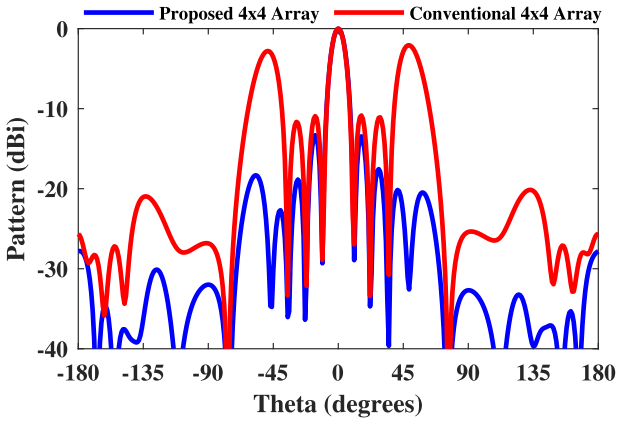

FIGURE 12. Comparison of the proposed 4 × 4 array with a fundamental mode 4 × 4 patch array having the same inter-element spacing of $1.3\lambda_0$.

an inter-element spacing of $1.3\lambda_0$ is plotted in Fig. 13a along with E- and H-plane patterns of the proposed antenna element. It can be seen from the array factor plot that the grating lobes are present at $\pm 45°$ due to inter-element spacing of $1.3\lambda_0$. However, these grating lobes are suppressed by the element patterns, which are about -20 dB down at the grating lobe locations. The undersampled array was simulated in HFSS, and its simulated radiation patterns are shown in Fig. 13b. The figure shows that the resultant pattern of the undersampled array does not have any grating lobes, and the SLL is about -13 dB down.

The grating lobe problem can also be avoided in a conventional patch array by reducing the inter-element spacing. For example, Fig. 14 shows an 8 × 8 array of fundamental mode patches having the same area as the proposed array with inter-element separation of $0.64\lambda_0$. However, it is worth mentioning that this reduction in the grating lobe is achieved at the expense of increased array

TABLE 2. Comparison of TM_{30} mode rectangular microstrip patch antennas.

Ref.	Freq (GHz)	Gain (dBi)	SLL(dB)	Sym. in Patterns	X-pol (dB)	BW (%)	Ap. Eff. (%)	Technique
[18]	3	13.3	-12.7	Yes	≤-30	0.7	81.02	Diff. Fed Slots
[22]	4.2	12.8	-20.8	Yes	≤-30	1.52	62.5	Slot Loading
[24]	3.55	13.7	-11.5	Yes	≤-40	12.4	52.03	Diff. Fed Slots
[25]	3.23	13.9	-10.8	Yes	-35	0.93	80.25	Notch-Loading
[26]	2.6	15	-6	No	-18.7	4.9	83.77	Notch-Loading
[27]	5.8	10.5	–	Yes	-18	6.7	52.5	Notch-Loading
Proposed	3.09	13.3	-16.1	Yes	-39	1.94	76.36	Notch-Loading with Fractal-Slot

Ref. = References ; Freq = Center Frequency; SLL = Sidelobe Level; X-pol = Cross-Polariztion; BW = Bandwidth; Ap. Eff. = Aperture Efficiency

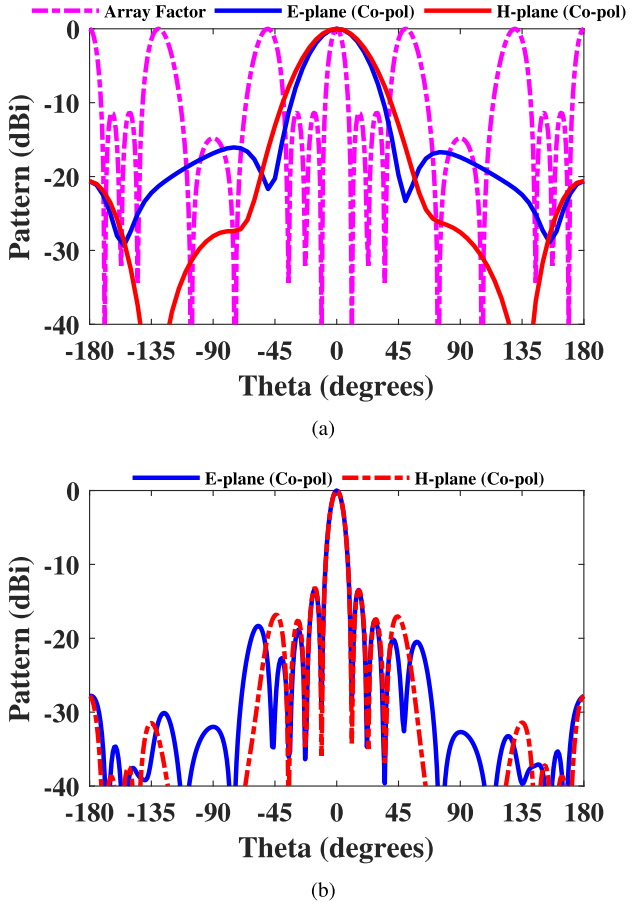

FIGURE 13. Radiation patterns of an array of the proposed antenna elements: (a) element pattern, corresponding array factor, and (b) resultant patterns.

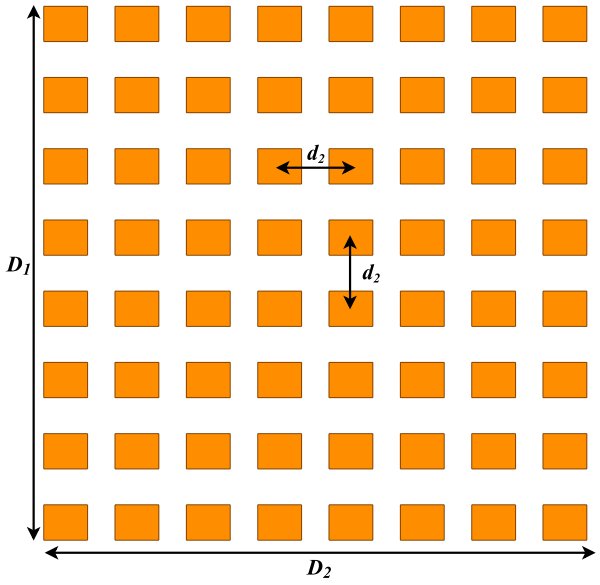

FIGURE 14. 8 × 8 fundamental mode array having the same area as the proposed array with inter-element spacing of $d_2 = 0.64\lambda_0$.

TABLE 3. Comparison of the undersampled array with an equivalent conventional array.

Parameter	Conventional Array	Undersampled Array
Area (λ_0^2)	23.6	23.9
Spacing (λ_0)	0.64	1.3
Elements	64	16
Gain (dBi)	25.5	25.4
SLL (dB)	-13	-13.1

elements. Thus, the proposed 4×4 undersampled array offers similar radiation characteristics compared to its conventional counterpart while reducing the number of elements by a factor of 4.

Table 3 compares both arrays in terms of the overall area, the number of elements, gain, SLL, and inter-element spacing. Both arrays have approximately the same area, and their gain is approximately 25.5 dBi, whereas the SLL is about 13 dB down. However, in the proposed undersampled array, the number of radiating elements is reduced by a factor of 4, reducing the feed complexity of the array and allowing more space to integrate other microwave components.

V. CONCLUSION

In this work, a high gain and low SLL TM_{30} mode patch is presented by combining the fractal-slot with notch-loading technique. It is shown that the fractal-slot loading technique can be used to remove the out-of-phase current distribution in TM_{30} mode, which in turn improves SLL, return loss and impedance bandwidth. When compared with a notch-loaded TM_{30} mode patch, the proposed antenna shows about 5 dB improvement in SLL with almost similar gain. Moreover, return loss is improved by 8 dB, and impedance bandwidth is increased by a factor of 2. In addition, symmetrical radiation patterns with X-pol levels of less than 35 dB are also achieved without using differential feeding. By utilizing the low SLL property of the proposed antenna, a 4×4 undersampled array

having a gain of 25 dBi and a simple feeding mechanism is also demonstrated for high gain applications. The proposed concept of fractal-slot and notch-loading can be extended to patch antennas with triangular or circular shapes.

REFERENCES

[1] D. M. Pozar, "Microstrip antennas," *Proc. IEEE*, vol. 80, no. 1, pp. 79–91, Jan. 1992.
[2] D. Pozar and D. Schaubert, *Microstrip Antennas: The Analysis and Design of Microstrip Antennas and Arrays*. Hoboken, NJ, USA: Wiley, 1995.
[3] E. Nishiyama, M. Aikawa, and S. Egashira, "Stacked microstrip antenna for wideband and high gain," *IEE Proc.-Microw., Antennas Propag.*, vol. 151, no. 2, pp. 143–148, Apr. 2004.
[4] R. Q. Lee and K.-F. Lee, "Experimental study of the two-layer electromagnetically coupled rectangular patch antenna," *IEEE Trans. Antennas Propag.*, vol. 38, no. 8, pp. 1298–1302, Aug. 1990.
[5] D. Jackson and N. Alexopoulos, "Gain enhancement methods for printed circuit antennas," *IEEE Trans. Antennas Propag.*, vol. AP-33, no. 9, pp. 976–987, Sep. 1985.
[6] H. Yang and N. Alexopoulos, "Gain enhancement methods for printed circuit antennas through multiple superstrates," *IEEE Trans. Antennas Propag.*, vol. AP-35, no. 7, pp. 860–863, Jul. 1987.
[7] A. P. Feresidis, G. Goussetis, S. Wang, and J. C. Vardaxoglou, "Artificial magnetic conductor surfaces and their application to low-profile high-gain planar antennas," *IEEE Trans. Antennas Propag.*, vol. 53, no. 1, pp. 209–215, Jan. 2005.
[8] A. Foroozesh and L. Shafai, "Investigation into the effects of the patch-type FSS superstrate on the high-gain cavity resonance antenna design," *IEEE Trans. Antennas Propag.*, vol. 58, no. 2, pp. 258–270, Feb. 2010.
[9] A. Pirhadi, H. Bahrami, and J. Nasri, "Wideband high directive aperture coupled microstrip antenna design by using a FSS superstrate layer," *IEEE Trans. Antennas Propag.*, vol. 60, no. 4, pp. 2101–2106, Apr. 2012.
[10] X. Zhang and L. Zhu, "Gain-enhanced patch antennas with loading of shorting pins," *IEEE Trans. Antennas Propag.*, vol. 64, no. 8, pp. 3310–3318, Aug. 2016.
[11] X. Zhang and L. Zhu, "High-gain circularly polarized microstrip patch antenna with loading of shorting pins," *IEEE Trans. Antennas Propag.*, vol. 64, no. 6, pp. 2172–2178, Jun. 2016.
[12] P. Juyal and L. Shafai, "A novel high-gain printed antenna configuration based on TM_{12} mode of circular disc," *IEEE Trans. Antennas Propag.*, vol. 64, no. 2, pp. 790–796, Feb. 2016.
[13] P. Juyal and L. Shafai, "A high-gain single-feed dual-mode microstrip disc radiator," *IEEE Trans. Antennas Propag.*, vol. 64, no. 6, pp. 2115–2126, Jun. 2016.
[14] P. Juyal and L. Shafai, "Gain enhancement in circular microstrip antenna via linear superposition of higher zeros," *IEEE Antennas Wireless Propag. Lett.*, vol. 16, pp. 896–899, 2016.
[15] P. Squadrito, S. Zhang, and G. F. Pedersen, "Wideband or dual-band low-profile circular patch antenna with high-gain and sidelobe suppression," *IEEE Trans. Antennas Propag.*, vol. 66, no. 6, pp. 3166–3171, Jun. 2018.
[16] S. Maci, G. Gentili, and G. Avitabile, "Single-layer dual frequency patch antenna, *Electron. Lett.*, vol. 29, no. 16, pp. 1441–1443, Aug. 1993.
[17] P. Juyal and L. Shafai, "Sidelobe reduction of TM_{12} mode of circular patch via nonresonant narrow slot," *IEEE Trans. Antennas Propag.*, vol. 64, no. 8, pp. 3361–3369, Aug. 2016.
[18] Z. Ahmed, M. M. Ahmed, and M. B. Ihsan, "A novel differential fed high gain patch antenna using resonant slot loading," *Radioengineering*, vol. 27, pp. 662–670, Sep. 2018.
[19] Q. U. Khan, D. Fazal, and M. B. Ihsan, "Use of slots to improve performance of patch in terms of gain and sidelobes reduction," *IEEE Antennas Wireless Propag. Lett.*, vol. 14, pp. 422–425, 2015.
[20] X. Zhang and L. Zhu, "Dual-band high-gain differentially fed circular patch antenna working in TM_{11} and TM_{12} modes," *IEEE Trans. Antennas Propag.*, vol. 66, no. 6, pp. 3160–3165, Jun. 2018.
[21] N.-W. Liu, L. Zhu, W.-W. Choi, and X. Zhang, "A low-profile differential-fed patch antenna with bandwidth enhancement and sidelobe reduction under operation of TM_{10} and TM_{12} modes," *IEEE Trans. Antennas Propag.*, vol. 66, no. 9, pp. 4854–4859, Sep. 2018.
[22] X. Zhang, L. Zhu, and Q.-S. Wu, "Sidelobe-reduced and gain-enhanced square patch antennas with adjustable beamwidth under TM_{03} mode operation," *IEEE Trans. Antennas Propag.*, vol. 66, no. 4, pp. 1704–1713, Apr. 2018.
[23] Y. He, Y. Li, W. Sun, and Z. Zhang, "Dual-polarized, high-gain, and low-profile magnetic current array antenna," *IEEE Trans. Antennas Propag.*, vol. 67, no. 2, pp. 1312–1317, Feb. 2019.
[24] X. Zhang, K.-D. Hong, L. Zhu, X.-K. Bi, and T. Yuan, "Wideband differentially fed patch antennas under dual high-order modes for stable high gain," *IEEE Trans. Antennas Propag.*, vol. 69, no. 1, pp. 508–513, Jan. 2021.
[25] Z. Ahmed and M. M. Ahmed, "Sidelobe reduction and gain enhancement in higher order TM_{30} and TM_{70} mode rectangular patch antennas via partial notch loading," *IET Microw., Antennas Propag.*, vol. 13, no. 12, pp. 1955–1962, Oct. 2019.
[26] J. Anguera, A. Andujar, and J. Jayasinghe, "High-directivity microstrip patch antennas based on TM_{odd-0} modes," *IEEE Antennas Wireless Propag. Lett.*, vol. 19, no. 1, pp. 39–43, Jan. 2020.
[27] A. Bhattacharyya, J. Pal, K. Patra, and B. Gupta, "Bandwidth-enhanced miniaturized patch antenna operating at higher order dual-mode resonance using modal analysis," *IEEE Antennas Wireless Propag. Lett.*, vol. 20, no. 2, pp. 274–278, Feb. 2021.
[28] C. A. Balanis, *Antenna Theory Analtsis Design*. Hoboken, NJ, USA: Wiley, 2016.
[29] J. Anguera, G. Montesinos, C. Puente, C. Borja, and J. Soler, "An undersampled high-directivity microstrip patch array with a reduced number of radiating elements inspired on the Sierpinski fractal," *Microw. Opt. Technol. Lett.*, vol. 3777, no. 2, pp. 100–103, Apr. 2003.

ZUBAIR AHMED received the B.Sc. and M.Sc. degrees in electrical engineering from the National University of Sciences and Technology (NUST), Pakistan, in 2003 and 2008, respectively, and the Ph.D. degree in electrical engineering from the Capital University of Science and Technology (CUST), Pakistan, in 2021. He joined the Department of Electrical Engineering, College of Electrical and Mechanical Engineering, NUST, in 2010. He is a Senior Member of the Microwave Engineering Research Laboratory (MERL). His current research interest includes high gain higher order mode patch antennas, transmit and reflectarray antennas, multibeam antennas, passive microwave circuits, and integrated RF front ends.

AWAB MUHAMMAD received the B.S. degree in electrical engineering from the National University of Sciences and Technology (NUST), Islamabad, Pakistan, in 2018, where he is currently pursuing the M.S. degree in electrical engineering.

Since 2018, he has been working with the Microwave Engineering Research Laboratory (MERL), NUST. His research interests include reflectarrays, transmitarrays, multi-beam antennas, DRAs, microstrip patch antennas, large frequency ratio antennas, and higher-order mode antennas.

MOJEEB BIN IHSAN received the B.Sc. degree in electrical engineering from the University of Engineering and Technology, Lahore, Pakistan, in 1984, and the M.Sc. and Ph.D. degrees in electrical engineering from Drexel University, Philadelphia, PA, USA, in 1988 and 1993, respectively.

In 1995, he joined the Department of Electrical Engineering, College of Electrical and Mechanical Engineering, National University of Sciences and Technology (NUST), Islamabad, Pakistan, where he has established the Microwave Engineering Research Laboratory (MERL) to conduct research and development in electronic systems, development of microwave and radar technology for biomedical applications, microwave active and passive circuits, antennas, radar signal processing, and target classification. He was the Head of the Department of Electrical Engineering, NUST, where he is currently a Professor, and the Director of MERL. His current research interests include solid-state electronics, thin-film processing, microwave devices and circuits, and antennas.